Theoretical analysis of velocity-selective Raman transitions

Kathryn Moler, David S. Weiss, Mark Kasevich, and Steven Chu
Physics Department, Stanford University, Stanford, California 94305
(Received 29 July 1991)

This paper analyzes the use of Raman transitions to select a narrow velocity distribution of atoms. We determine the evolution of the atomic wave function comprised of both the internal state and the external momentum of the atom in the presence of two counterpropagating laser beams. The effects of a single π pulse, two separated Ramsey $\pi/2$ pulses, and a sequence of four $\pi/2$ pulses are analyzed.

PACS number(s): 32.80.Pj, 42.50.Vk

I. INTRODUCTION

Laser cooling of atoms relies on repeated cycles of stimulated absorption and spontaneous emission to dissipate atomic energy. When an atom of mass M spontaneously emits a photon of wave number k, it acquires a randomly oriented recoil velocity $v_R = \hbar k/M$. Because of this heating process, the recoil velocity is a potential limit to the velocity spreads that may be reached with laser cooling. For instance, optical molasses can cool atoms to a few times the recoil limit [1].

It is natural to consider how one might cool below the recoil limit. One way is to bind the atom to a massive object, such as an ion trap, which absorbs the recoil momentum of the photon. The "sideband cooling" of ions in an ion trap [2] circumvents the recoil limit in this way, but is not feasible for neutral atoms at present. Another possibility is the coherent-population-trapping technique of Aspect *et al.* [3], which can cool atoms with a $J=1$ to $J=1$ transition far below the recoil limit.

In this paper, we will analyze a method of selecting an ensemble of atoms with a very well-defined velocity. This type of velocity selection does not increase the number of atoms with a given velocity, and is therefore not a cooling technique. The method uses a stimulated Raman transition with the two laser beams counterpropagating, so that the transition is Doppler sensitive. To understand how stimulated Raman transitions are used for velocity selection, consider an atom with an optical transition and a ground-state hyperfine splitting. After being optically pumped into a single hyperfine level $|1\rangle$, the atom is irradiated with two counterpropagating "velocity selection" beams of frequencies ω_{1L} and ω_{2L}. If an atom has a velocity component v_x parallel to the laser beams such that $\omega_{1L}-\omega_{2L}$ is Doppler shifted so as to be in resonance with the hyperfine splitting of the ground state, it will be driven from state $|1\rangle$ to state $|2\rangle$. The velocity spread Δv_x of the excited atoms is related to the Raman linewidth $\Delta\omega$ by the Doppler-shift formula,

$$\frac{\Delta v_x}{c}=\frac{\Delta\omega}{\omega_{IL}+\omega_{2L}} . \tag{1}$$

Under certain conditions, the linewidth of the Raman transition will be measurement-time limited; Ezekiel and co-workers have demonstrated a 1.3-kHz measurement-time limited Raman linewidth [4]. This linewidth can be further reduced using the longer measurement times available with laser cooling. We have previously shown that a 5-cm-high fountain of laser-cooled atoms with a measurement time of 0.25 s gives a 2-Hz linewidth [5]. Such narrow linewidths permit velocity selection far below the recoil limit. For a velocity-sensitive Raman transition with 589-nm light, a linewidth of 100 Hz corresponds to a velocity width of 29 μm/s. For comparison, the recoil velocity of sodium is 3 cm/s.

Raman velocity selection of sodium atoms has been demonstrated with a full width at half maximum (FWHM) of 25 Hz, corresponding to a velocity width of 7 μm/s [6]. In that work, we also showed how the Raman velocity selection can be used to measure ultralow temperatures when ballistic methods fail. We present here a theoretical treatment of the velocity-sensitive Raman transition, and consider some of the limits to the velocity resolution. Because of the large uncertainty in the position of an atom with such a well-defined velocity, the atom's center-of-mass coordinates cannot be treated classically. The full quantum-mechanical treatment presented here uses the method of closed-momentum families, as developed by Aspect *et al.*, to analyze coherent population trapping [7].

In Sec. II, we determine the evolution of the atomic wave function in the presence of the velocity-selection beams. We use this evolution to discuss some of the uses of velocity-selective Raman transitions in Sec. III.

II. MOMENTUM-DEPENDENT EVOLUTION OF THE SYSTEM

A. Statement of the problem

Consider an atom that has the level scheme shown in Fig. 1, with a ground-state hyperfine interval ω_{21} and an optical interval ω_{31}. The atom is irradiated with counterpropagating laser beams of frequencies ω_{1L} and ω_{2L}. The states are labeled by both their internal quantum numbers and their momenta parallel to the laser beams. Thus the notation $|1,p-\hbar k_{1L}\rangle$ indicate that the atom has momentum $p-\hbar k_{1L}$ parallel to the laser beams and that it is in internal state $|1\rangle$. For a transition from an initial state $|1,p-\hbar k_{1L}\rangle$ to a final state $|2,p+\hbar k_{2L}\rangle$, the intermediate state is $|3,p\rangle$ as shown in Fig. 1.

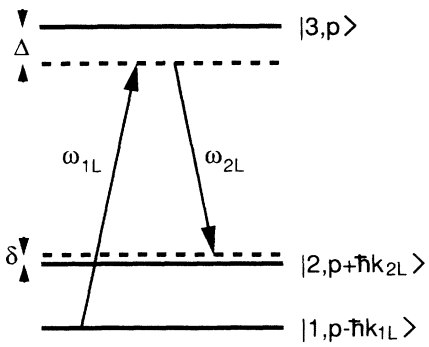

FIG. 1. A stimulated Raman transition within a momentum family p. For counterpropagating photons, δ is strongly momentum dependent.

We consider the time evolution of the wave function describing a single momentum family

$$|\Psi_p(t)\rangle = C_1(p,t)|1,p-\hbar k_{1L}\rangle + C_2(p,t)|2,p+\hbar k_{2L}\rangle + C_3(p,t)|3,p\rangle \ , \tag{2}$$

with the normalization $\langle\psi_p(t)|\psi_p(t)\rangle = 1$, in the limit where spontaneous emission can be ignored. In this limit, the states $|1,p-\hbar k_{1L}\rangle$, $|2,p+\hbar k_{2L}\rangle$, and $|3,p\rangle$ form a closed-momentum family labeled by p.

B. The equations of motion

Before quantizing the external momentum, the Hamiltonian is $H = H_A + H_{\rm int}$. The atomic Hamiltonian is

$$H_A = \frac{P^2}{2M} + \hbar\omega_{31}|3\rangle\langle 3| + \hbar\omega_{21}|2\rangle\langle 2| \ , \tag{3}$$

and the interaction Hamiltonian is

$$H_{\rm int} = -\mathbf{d}\cdot\mathbf{E}(x,t) \ , \tag{4}$$

where $\mathbf{d}$ is the electric dipole moment operator. The electric field is two traveling waves $\mathbf{E}_1$ and $\mathbf{E}_2$ counterpropagating along x. The total field is

$$\mathbf{E}(x,t) = \tfrac{1}{2}\mathbf{E}_1 e^{i(k_{1L}x-\omega_{1L}t)} + \tfrac{1}{2}\mathbf{E}_2 e^{-i(-k_{2L}x-\omega_{2L}t)} + \text{c.c.} \tag{5}$$

We assume that $\mathbf{E}_1$ only couples states $|1\rangle$ and $|3\rangle$ while $\mathbf{E}_2$ only couples states $|2\rangle$ and $|3\rangle$. This assumption can be rigorously true for some atomic-level configurations and photon polarizations, and is a good approximation if the hyperfine splitting is much larger than the detunings from the optical transitions. Defining the Rabi frequencies Ω_1 and Ω_2 as

$$\Omega_n = -\frac{\langle n|\mathbf{d}\cdot\mathbf{E}_n|3\rangle}{2\hbar} \ , \quad n = 1,2 \tag{6}$$

the interaction Hamiltonian is

$$H_{\rm int} = \hbar\Omega_1^* e^{i(k_{1L}x-\omega_{1L}t)}|3\rangle\langle 1| + \hbar\Omega_2^* e^{i(-k_{2L}x-\omega_{2L}t)}|3\rangle\langle 2| + \text{c.c.} \tag{7}$$

Substituting the relation

$$e^{\pm ikx} = \int |p\rangle\langle p \mp \hbar k|\,dp \tag{8}$$

into Eq. (7) shows that absorption or emission of a photon of wave number k changes the atom's total momentum by an amount $\hbar k$. Thus the velocity-selection beams only induce transitions within a closed-momentum family, as described above. The time evolution of the coefficients $C_i(p,t)$, $i = 1,2,3$, is determined by the Hamiltonian

$$H = \begin{bmatrix} \dfrac{(p-\hbar k_{1L})^2}{2M} & 0 & \hbar\Omega_1 e^{i\omega_{1L}t} \\ 0 & \dfrac{(p+\hbar k_{2L})^2}{2M} + \hbar\omega_{21} & \hbar\Omega_2 e^{i\omega_{2L}t} \\ \hbar\Omega_1^* e^{-i\omega_{1L}t} & \hbar\Omega_2^* e^{-i\omega_{2L}t} & \dfrac{p^2}{2M} + \hbar\omega_{31} \end{bmatrix} . \tag{9}$$

This equation is similar to the Hamiltonian derived by Aspect *et al.*, to treat coherent population trapping [7]. In fact, for $\omega_{1L} = \omega_{2L}$, $\omega_{12} = 0$, and proper choice of the angular momenta of the lasers and the ground state, Eq. (9) is equivalent to the Hamiltonian derived in Sec. 3B of Ref. [7].

We define B_i, $i = 1,2,3$, as

$$B_1(p,t) = C_1(p,t)\exp\left[i\frac{(p-\hbar k_{1L})^2}{2M\hbar}t\right] , \tag{10a}$$

$$B_2(p,t) = C_2(p,t)\exp\left[i\left[\frac{(p+\hbar k_{2L})^2}{2M\hbar} + \omega_{21}\right]t\right] , \tag{10b}$$

$$B_3(p,t) = C_3(p,t)\exp\left[i\left[\frac{p^2}{2M\hbar} + \omega_{31}\right]t\right] . \tag{10c}$$

The detuning δ of $\omega_{1L}-\omega_{2L}$ from the transition $|1,p-\hbar k_{1L}\rangle \rightarrow |2,p+\hbar k_{2L}\rangle$ is

$$\delta \equiv \left[\frac{(p-\hbar k_{1L})^2}{2M\hbar} - \omega_{21} - \frac{(p+\hbar k_{2L})^2}{2M\hbar}\right] - (\omega_{2L}-\omega_{1L})$$

$$= -\frac{p(k_{1L}+k_{2L})}{M} + \left[\frac{(\hbar k_{1L}^2)}{2M} - \frac{(\hbar k_{2L}^2)}{2M}\right] - \omega_{21} - (\omega_{2L}-\omega_{1L}) \ . \tag{11a}$$

This definition includes the laser frequencies, the Doppler shift, and the recoil energies. The detuning Δ of ω_{1L} from the transition $|1,p-\hbar k_{1L}\rangle \rightarrow |3,p\rangle$ is defined as

$$\Delta \equiv \left[\frac{p^2}{2M\hbar} + \omega_{31} - \frac{(p-\hbar k_{1L})^2}{2M\hbar}\right] - \omega_{1L}$$

$$= \frac{pk_{1L}}{M} - \frac{\hbar k_{1L}^2}{2M} + \omega_{31} - \omega_{1L} \ . \tag{11b}$$

The detuning of ω_{2L} from the transition $|2,p+\hbar k_{2L}\rangle \rightarrow |3,p\rangle$ is given by $\Delta+\delta$. With these definitions, the equations of motion are

$$\frac{dB_1}{dt} = -i\Omega_1 e^{-i\Delta t} B_3 \ , \tag{12a}$$

$$\frac{dB_2}{dt} = -i\Omega_2 e^{-i(\Delta+\delta)t} B_3 \ , \tag{12b}$$

$$\frac{dB_3}{dt} = -i\Omega_i^* e^{i\Delta t} B_1 - i\Omega_2^* e^{i(\Delta+\delta)t} B_2 \ . \tag{12c}$$

C. Solution of the equations

Because δ is sensitive to the first-order Doppler shift of twice an optical-photon frequency and the linewidth of the Raman transition is narrow, only a narrow class of momentum families is resonant with the stimulated Raman transition. If the momentum family $p = p_0$ satisfies the Raman resonance condition, i.e.,

$$\omega_{2L} - \omega_{1L} = \frac{(p_0 - \hbar k_{1L})^2}{2M\hbar} - \omega_{21} - \frac{(p_0 + \hbar k_{2L})^2}{2M\hbar} \ , \tag{13}$$

then the detuning for an arbitrary momentum family p is $\delta = -(p - p_0)(k_{1L} + k_{2L})/M$. Equation (12) may be solved exactly, following Brewer and Hahn [8], for the special case $\delta = 0$. However, we are also interested in the coefficients for $\delta \neq 0$, when the atoms are Doppler shifted out of resonance.

In order to suppress spontaneous emission, the detuning from the optical transition Δ is made large. With the conditions

$$\Delta \gg |\Omega_1|, |\Omega_2|, \delta \ , \tag{14}$$

the three-level equations [Eqs. (12)] may be reduced to analytically soluble two-level equations. We assume, and verify by the solutions, that the coefficients B_1 and B_2 oscillate much more slowly than the detuning Δ. Equation (12c) may be integrated directly by ignoring the time dependence of B_1 and B_2, making errors of order $T\Omega^3/\Delta^2$ and order $t\Omega^2\delta/\Delta^2$. The result is substituted into (12a) and (12b). Terms that oscillate at frequency Δ are neglected, since they quickly average out to give a negligible contribution to B_1 and B_2. The resulting effective two-level equations are

$$\frac{dB_1}{dt} = i\frac{|\Omega_1|^2}{\Delta} B_1 + i\frac{\Omega_1\Omega_2^*}{\Delta} B_2 e^{i\delta t} \ , \tag{15a}$$

$$\frac{dB_2}{dt} = i\frac{\Omega_1^*\Omega_2}{\Delta} B_1 e^{-i\delta t} + i\frac{|\Omega_2|^2}{\Delta} B_2 \ . \tag{15b}$$

The solutions to these equations are [9]

$$B_1(p, t_0+t) = \exp\left[i\left[\delta + \frac{|\Omega_1|^2}{\Delta} + \frac{|\Omega_2|^2}{\Delta} \right] \frac{t}{2} \right] \times \left\{ \left[\cos\frac{\omega t}{2} + \frac{i}{\omega}\left[\frac{|\Omega_1|^2}{\Delta} - \frac{|\Omega_2|^2}{\Delta} - \delta \right] \sin\left[\frac{\omega t}{2} \right] \right] B_1(p, t_0) + \frac{i}{\omega}\frac{2\Omega_1\Omega_2^*}{\Delta} \sin\left[\frac{\omega t}{2} \right] e^{i\delta t_0} B_2(p, t_0) \right\} , \tag{16a}$$

$$B_2(p, t_0+t) = \exp\left[i\left[-\delta + \frac{|\Omega_1|^2}{\Delta} + \frac{|\Omega_2|^2}{\Delta} \right] \frac{t}{2} \right] \left\{ \frac{i}{\omega}\frac{2\Omega_1^*\Omega_2}{\Delta} \sin\left[\frac{\omega t}{2} \right] e^{-i\delta t_0} B_1(p, t_0) + \left[\cos\left[\frac{\omega t}{2} \right] - \frac{i}{\omega}\left[\frac{|\Omega_1|^2}{\Delta} - \frac{|\Omega_2|^2}{\Delta} - \delta \right] \sin\left[\frac{\omega t}{2} \right] \right] B_2(p, t_0) \right\} , \tag{16b}$$

where

$$\omega^2 = \left[\frac{|\Omega_1|^2}{\Delta} - \frac{|\Omega_2|^2}{\Delta} - \delta \right]^2 + 4\frac{|\Omega_1|^2|\Omega_2|^2}{\Delta^2} \ . \tag{17}$$

The second term in Eq. (17) is the square of the two-photon Rabi frequency. The first term contains the momentum-dependent detuning δ, as well as the ac Stark shifts $|\Omega_1|^2/\Delta$ and $|\Omega_2|^2/\Delta$, to zeroth order in δ/Δ.

The approximate validity of these solutions is verified by substitution back into the original three-level equations. We have also solved Eq. (12) numerically, and find a good agreement with Eqs. (16) and (17) when Eq. (14) is satisfied.

III. APPLICATIONS OF THE SOLUTIONS

A. Velocity-selective π pulse

Consider a wave packet that is a superposition of momentum families,

$$|\Psi(t)\rangle = \int g(p) |\psi_p(t)\rangle dp \ , \tag{18}$$

where

$$|\psi_p(t)\rangle = C_1(p,t)|1, p - \hbar k_{1L}\rangle + C_2(p,t)|2, p + \hbar k_{2L}\rangle$$

as in Eq. (2), and $|g(p)|^2$ is the probability of finding the atom in the momentum family p, i.e., in either the state $|1, p - \hbar k_{1L}\rangle$ or the state $|2, p + \hbar k_{2L}\rangle$. The distribution

$g(p)$ is normalized separately from $|\psi_p(t)\rangle$ so that

$$\int |g(p)|^2 dp = 1 \ . \tag{19}$$

Since there is negligible redistribution between momentum families under our conditions, $g(p)$ is time independent.

As an example, consider an ensemble of atoms optically pumped into the $|1\rangle$ state, $C_1(p,0)=1$, with a Gaussian distribution of momenta

$$g(p)=\pi^{-1/4}\sigma_p^{-1/2}\exp\left[-\frac{(p-p_0)^2}{2\sigma_p^2}\right], \tag{20}$$

where p_0 is the center of the momentum family distribution and σ_p is its width. Since the ensemble is in state $|1\rangle$, its center velocity is $(p_0-\hbar k_{1L})/M$. After a time τ, the momentum-dependent probabilities $P_1(p)$ and $P_2(p)$ of occupying the internal states $|1\rangle$ and $|2\rangle$, respectively, are

$$\begin{aligned} P_1(p)&=|g(p)C_1(p,\tau)|^2 \\ &=\frac{1}{\sqrt{\pi}\sigma_p}\exp\left[-\frac{(p-p_0)^2}{\sigma_p^2}\right] \\ &\times\left[\cos^2\left[\frac{\omega\tau}{2}\right]+\frac{1}{\omega^2} \right. \\ &\left.\times\left[\frac{|\Omega_1|^2}{\Delta}-\frac{|\Omega_2|^2}{\Delta}-\delta\right]^2\sin^2\left[\frac{\omega\tau}{2}\right]\right], \end{aligned} \tag{21a}$$

$$\begin{aligned} P_2(p)&=|g(p)C_2(p,\tau)|^2 \\ &=\frac{4|\Omega_1|^2|\Omega_2|^2}{\sqrt{\pi}\sigma_p\omega^2\Delta^2}\exp\left[-\frac{(p-p_0)^2}{\sigma_p^2}\right]\sin^2\left[\frac{\omega\tau}{2}\right]. \end{aligned} \tag{21b}$$

Equations (21a) and (21b) are plotted in Fig. 2 for a π pulse. Note that a net momentum of twice the one-photon recoil momentum is imparted to the state $|2\rangle$ in completing the hyperfine transition.

B. Ramsey-Raman velocity selection

If a narrow velocity slice is selected out of the initial velocity distribution, most of the atoms would not contribute to the counting rate of an experiment. However, for a number of experiments, such as the search for a small charge imbalance on an atom, a collection of many narrow velocity slices selected out of the original distribution may be used [10]. One way to select a number of narrow velocity classes is to impose several frequency sidebands on one of the laser beams. This method has the practical disadvantage of increasing the probability of spontaneous-emission events. Another way to create many peaks of velocity-selected atoms is to use Ramsey's method of separated oscillatory fields [10,11]. After being pumped into level $|1\rangle$, the atoms are given two $\pi/2$ pulses of length τ separated by a time T. The probability of transition to level $|2\rangle$ is

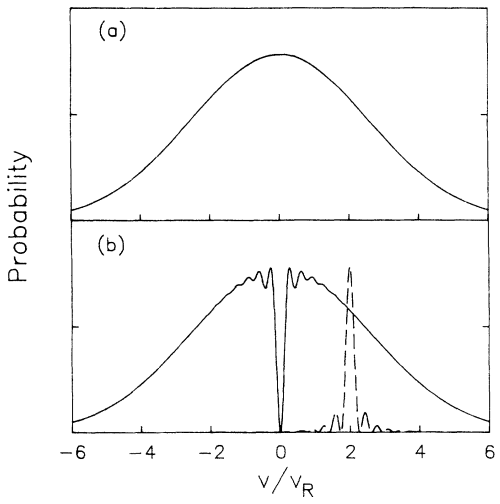

FIG. 2. A velocity-selective Raman π pulse, with $\sigma_p=3.6mv_R/\sqrt{2}$, $\tau=10/kv_R$, and $\Omega_1\Omega_2/\Delta=0.16kv_R$. (a) Initial momentum distribution in state $|1\rangle$. (b) Final momentum distribution. The sold line represents state $|1\rangle$ and the dashed line represents state $|2\rangle$.

$$\begin{aligned} |C_2(p,T+2\tau)|^2&=\frac{16|\Omega_1|^2|\Omega_2|^2}{\omega^2\Delta^2}\sin^2\left[\frac{\omega\tau}{2}\right] \\ &\times\left[\cos\left[\frac{\omega\tau}{2}\right]\cos\left[\frac{\delta T}{2}\right]+\frac{1}{\omega}\right. \\ &\times\left[\frac{|\Omega_1|^2}{\Delta}-\frac{|\Omega_2|^2}{\Delta}-\delta\right] \\ &\left.\times\sin\left[\frac{\omega\tau}{2}\right]\sin\left[\frac{\delta T}{2}\right]\right]^2. \end{aligned} \tag{22}$$

$P_1(p)=|g(p)C_1(p,t)|^2$ and $P_2(p)=|g(p)C_2(p,t)|^2$ are shown in Fig. 3, with $g(p)$ given by Eq. (20). Each velocity selected group has a width $\lambda/4T$, where λ is the wavelength of the light, and the width of the envelope is $\lambda/2\tau$.

Ramsey-Raman velocity selection is particularly useful for experiments in which the effect being studied induces an identical velocity change for all velocity groups. The velocity change would be measured by using two separated pairs of $\pi/2$ pulses. Consider an ensemble of atoms beginning in the $|1\rangle$ state. After the application of the first set of $\pi/2$ pulses, a Ramsey fringe pattern will be established in v_x velocity space as shown in Fig. 3. Assume there is a perturbation that shifts all v_x velocities by an amount Δv_x before the application of the second $\pi/2$ pulse sequence. The number of atoms that can be found in the $|1\rangle$ state as a function of Δv_x is plotted in Fig. 4. In the calculation of Fig. 4, we have assumed that the $\pi/2$ pulse duration τ is sufficiently short that the Ramsey velocity structure (the velocity "picket fence") shown in Fig. 3 extends over the entire initial velocity distribution. We have also assumed that the pulse duration τ will be the same for all atoms (implemented by pulsing the laser beams).

For velocity selection in a continuous atomic beam, τ

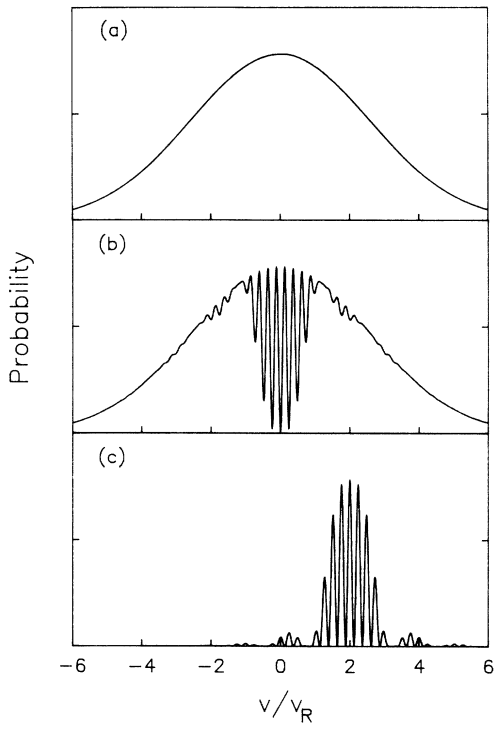

FIG. 3. A velocity-selective Ramsey-Raman transition, with $\sigma_p = 3.6mv_R/\sqrt{2}$, $\tau = 2.5/kv_R$, $T = 10/kv_R$, and $\Omega_1\Omega_2/\Delta = 0.16kv_R$. (a) Initial momentum distribution in state $|1\rangle$. (b) Final momentum distribution in state $|1\rangle$. (c) Final momentum distribution in state $|2\rangle$.

and T are determined by the axial velocity v_z of the atoms as they traverse the laser beams. When averaged over the axial velocity spread δv_z, the Ramsey pattern will be smoothed as shown in Fig. 5. Contrast is lost (in the limit where $\tau \ll T$) because atoms with different velocities have different Ramsey fringe spacings. The number of fringes that can be created is approximately $v_z/\delta v_z$. For cesium in an atomic fountain with polarization gradient cooling, $v_z \approx 1$ m/s and δv_z can be as low as a few times the recoil velocity 0.3 cm/s, so that $v_z/\delta v_z \approx 100$.

The loss of fringe contrast due to the different fringe spacings shown in Fig. 5 does not set a limit to the number of atoms within the velocity distribution that can be used in an experiment that measures small velocity changes. Consider an ensemble of atoms with a given v_z but with the full distribution of velocities v_x. The first set of $\pi/2$ pulses "writes" a Ramsey fringe pattern in the v_x velocity space of the atoms with a spacing between Ramsey fringes of $\lambda/2T$. When the second set of $\pi/2$ pulses is used to read out the fringes, the "readout spacing" is still $\lambda/2T$. A set of atoms with different velocity v_z' will have a different Ramsey spacing $\lambda/2T'$, but the "readout" spacing will always match the "written" spacing for each group of atoms. Thus the experimental contrast (e.g., the variation in the number of atoms in the $|2\rangle$ state) is not degraded by the difference in the times T and T'.

There will be a slight loss in contrast because atoms moving slower (or faster) than the average velocity will experience pulses greater (or less) than $\pi/2$ as they pass through the laser beams. If an atom of velocity $\langle v_z \rangle$ experiences a $\pi/2$ pulse, an atom with velocity $\langle v_z \rangle - \delta v_z$

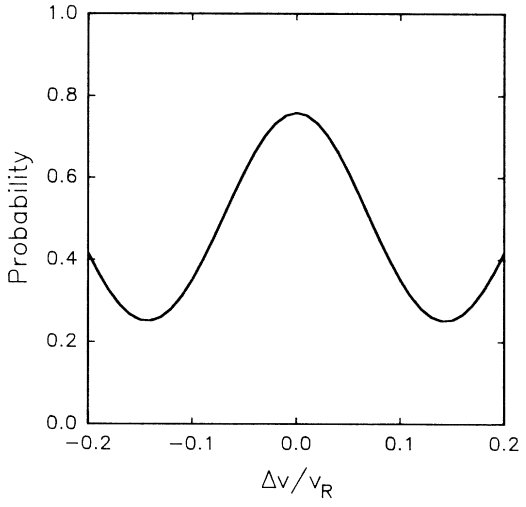

FIG. 4. The total probability, summed over all velocity classes, for an atom to be in the initial state after four $\pi/2$ pulses when a velocity change Δv is induced before the second pair of $\pi/2$ pulses. The parameters chosen are $\tau = 0.26/kv_R$ and $T = 20\tau$, and the initial transverse velocity distribution is narrow enough that all transverse velocity classes are in the excitation envelope.

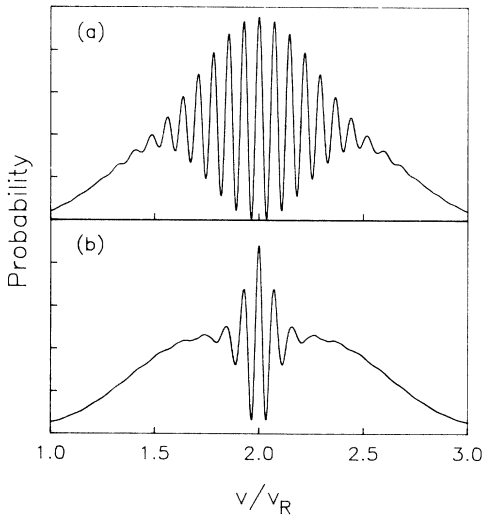

FIG. 5. Ramsey-Raman velocity selection on the transverse velocity in an atomic beam, averaged over the longitudinal velocity. For this figure, $\Omega_1\Omega_2/\Delta = 0.30kv_R$. $\tau = 2.5/kv_R$ and $T = 40/kv_R$ for the center of the longitudinal velocity distribution. The quantity shown is $|C_2(p)|^2$, averaged over v_z, for (a) $v_z/\sigma(v_z) = 20$, and (b) $v_z/\sigma(v_z) = 5$.

experiences a pulse $\pi/2-\epsilon$, where $\epsilon/(\pi/2)=\delta v_z/\langle v_z\rangle$. The loss of contrast is therefore not significant as long as δv_z is not a significant fraction of $\langle v_z\rangle$.

C. Spatial wave functions and interferometry

The spatial wave function of the atom is given by the Fourier transform of the momentum wave function. Assuming that the atom is in a wave packet of the form of Eq. (18), the external spatial wave functions $\phi_1(x,t)$ and $\phi_2,(x,t)$ associated with the internal states $|1\rangle$ and $|2\rangle$, respectively, are given by

$$\phi_1(x,t)=\frac{1}{\sqrt{2\pi\hbar}}\int_{-\infty}^{+\infty} g(p)C_1(p,t)e^{i(p-\hbar k_{1L})x/\hbar}dp\ , \tag{23a}$$

$$\phi_2(x,t)=\frac{1}{\sqrt{2\pi\hbar}}\int_{-\infty}^{+\infty} g(p)C_2(p,t)e^{i(p+\hbar k_{2L})x/\hbar}dp\ . \tag{23b}$$

As a test case, we assumed a $g(p)$ that describes a Gaussian wave packet [see Eq. (20)] that was initially limited by the uncertainty principle. We followed its evolution through a π pulse, two $\pi/2$ pulses, and a $\pi/2$, π, $\pi/2$ pulse sequence. Unlike our calculation of the velocity distribution, the calculation of the spatial wave functions depends on the phase relationship of the different momentum components. The center of mass of the state-$|1\rangle$ population moved with velocity $(p_0-\hbar k_{1L})/M$, and the state-$|1\rangle$ population's spatial width increased at a rate of σ_p/M from the original width. Similarly, the state-$|2\rangle$ population moved with a center velocity of $(p_0+\hbar k_{2L})/M$. The spreading of the state-$|2\rangle$ population was determined by the selected velocity width. Furthermore, when a narrow velocity group of atoms with width Δv_x was transferred to state $|2\rangle$, a spatial hole in the state-$|1\rangle$ population became visible after enough time had passed that $\Delta v_x t$ was larger than the initial spatial width.

The correlation between an atom's internal state and its momentum state makes the construction of an atomic interferometer possible. This has been discussed by Bordé [12] and recently demonstrated by Helmcke and co-workers [13]. Instead of using transitions between ground and excited states, we have proposed and demonstrated an atomic interferometer made by interfering different hyperfine ground states (Fig. 6) [14]. A related standing-wave interferometer based on a Raman transition has been analyzed by Marte, Cirac, and Zoller [15].

The interferometer begins with an atom, initially in the state $|1\rangle$. The center of the spatial distribution of such an atom is indicated by the solid line of Fig. 6. The atom is given a $\pi/2$ pulse, separating it into a state-$|1\rangle$ component with a momentum centered about $p_x-\hbar k_{1L}$ and a state $|2\rangle$ (dotted line) with a momentum centered about $p_x+\hbar k_{2L}$. After a time T, the atom evolves into two spatially separated, but coherent, wave packets that are labeled by their internal state. A π pulse at time T will put the part of the atom in state $|1\rangle$ centered about $p_x-\hbar k_{1L}$ into the state $|2\rangle$ centered about $p_x+\hbar k_{2L}$, and vice versa. Thus, the two separated states of the atom will begin to move towards each other. A final $\pi/2$ pulse is used to complete the interferometer, and depending on the phase of the second $\pi/2$ pulse relative to the other pulses, the atom can be put into either the $|1\rangle$ or $|2\rangle$ state.

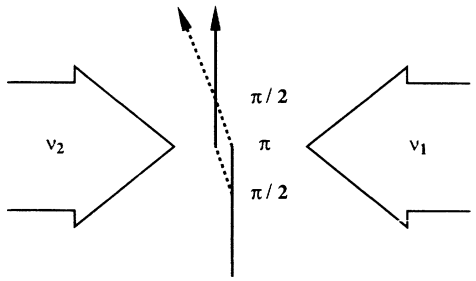

FIG. 6. Schematic of an atomic interferometer with a $\pi/2$-π-$\pi/2$ pulse sequence. The solid line indicates the center of the state $|1\rangle$ components and the dashed line indicates the center of the state $|2\rangle$ components.

There are two major advantages to using a Raman transition between ground states of an atom instead of using a single-photon transition as suggested by Bordé. First, the two frequencies v_1 and $v_2=v_1+v_{\rm rf}$ used in the Raman transition are derived from one laser and an electro-optic modulator so that the frequency and phase stability of the transition has the inherent stability of the rf source used to drive the modulator. Since the frequency jitter of the laser does not affect the measurement, radio-frequency control of the Raman transition can be obtained with a laser of modest frequency stability while the velocity recoil is twice the recoil resulting from an optical photon. Second, since the ground states are stable against decay, large time intervals between velocity-changing impulses are allowed, making possible interferometers with large spatial separations.

For atomic interferometers with long measurement times (as in an atomic-fountain geometry) it is important that the states be insensitive to perturbations in the magnetic field. Transitions with $m_F=0\rightarrow m_F'=0$ have been used in the works of the Physikalische-Technische Bundesanstalt [13] and Kasevich and Chu [14].

IV. CONCLUSIONS

The use of Raman transitions as a means of velocity selection has been analyzed in the Schrödinger picture. In this work, the combined effect on both the internal-energy state and the correlated-external-momentum state of an atom has been analyzed for a single π pulse, two $\pi/2$ pulses, two sets of $\pi/2$ pulses, and a $\pi/2$-π-$\pi/2$ pulse sequence for a distribution of atomic velocities. Under the experimental conditions where the laser detuning Δ is much larger than both the Rabi frequencies Ω_1 and Ω_2 of the two laser fields and the Doppler width of the atomic distribution, the two-photon transition between three levels can be reduced to an easily soluble set of two-level equations.

We have applied those solutions to study the effects of

pulses and pulse sequences that were first used in nuclear-magnetic-resonance studies of spin systems. Because the excitation of the transition depends on the frequency and phase difference of two laser frequencies that can be derive from a single laser, radio-frequency control of the transition is possible. Also, since the transitions are between hyperfine levels of the ground state, spontaneous emission is not a factor. Thus, we anticipate that many of the powerful NMR techniques first developed for two-level spin systems can be used in the mechanical manipulation of atoms.

ACKNOWLEDGMENTS

This work was supported in part by grants from the NSF and AFOSR. K.A.M. received additional support from the NSF and M.A.K. received support from IBM. We wish to thank E. Riis for helpful discussions.

[1] P. Lett, R. N. Watts, C. I. Westbrook, W. D. Phillips, P. L. Gould, and H. J. Metcalf, Phys. Rev. Lett. **61**, 169 (1988); J. Dalibard and C. Cohen-Tannoudji, J. Opt. Soc. Am. B **6**, 2023 (1989); D. S. Weiss, E. Riis, Y. Shevy, P. J. Ungar, and S. Chu, **6**, 2072 (1989); P. J. Ungar, D. S. Weiss, E. Riis, S. Chu, *ibid.* **6**, 2058 (1989); P. D. Lett, W. D. Phillips, S. L. Rolston, C. E. Tanner, R. N. Watts, and C. I. Westbrook, *ibid.* **6**, 2084 (1989).

[2] F. Diedrich, J. C. Berquist, W. Itano, and D. J. Wineland, Phys. Rev. Lett. **62**, 403 (1989).

[3] A. Aspect, E. Arimondo, R. Kaiser, N. Vansteenkiste, and C. Cohen-Tannoudji, Phys. Rev. Lett. **621**, 826 (1988).

[4] J. E. Thomas, P. R. Hemmer, S. Ezekiel, C. C. Leiby, Jr., P. H. Picard, and C. R. Willis, Phys. Rev. Lett. **48**, 867 (1982).

[5] M. Kasevich, E. Riis, S. Chu, and R. DeVoe, Phys. Rev. Lett. **63**, 612 (1989).

[6] M. Kasevich, D. S. Weiss, E. Riss, K. Moler, S. Kasapi, and S. Chu, Phys. Rev. Lett. **66**, 2297 (1991). In that publication, we reported a velocity spread of 270 μm/s, but in subsequent work by M. Kasevich and S. Chu, the 7-μm/s velocity spreads have been achieved.

[7] A. Aspect, E. Arimondo, R. Kaiser, N. Vansteenkiste, and C. Cohen-Tannoudji, J. Opt. Soc. Am. B **6**, 2112 (1989).

[8] R. G. Brewer and E. L. Hahn, Phys. Rev. A **11**, 1641 (1975).

[9] See for example N. F. Ramsey, Phys. Rev. **78**, 695 (1950).

[10] M. Kasevich, K. Moler, E. Riis, E. Sunderman, D. S. Weiss, and S. Chu, in *Atomic Physics 12*, edited by R. Lewis (AIP, New York, 1991), p. 47.

[11] E. V. Baklanov, B. Ya. Dubetsky, and V. P. Chebotayev, Appl. Phys. **9**, 171 (1976).

[12] Ch. J. Bordé, Phys. Lett. A **140**, 10 (1989).

[13] F. Riehle, Th. Kisters, A. Witte, J. Helmcke, and Ch. J. Bordé, Phys. Rev. Lett. **67**, 177 (1991).

[14] M. Kasevich and S. Chu, Phys. Rev. Lett. **67**, 181 (1991).

[15] M. Marte, J. I. Cirac, and P. Zoller J. Mod. Opt. (to be published).